



Tool wear mechanisms in axial ultrasonic vibration assisted milling in-situ TiB₂/7050Al metal matrix composites

Xiao-Fen Liu¹ · Wen-Hu Wang¹ · Rui-Song Jiang² · Yi-Feng Xiong¹ · Kun-Yang Lin¹

Received: 22 July 2019 / Revised: 2 October 2019 / Accepted: 27 January 2020 / Published online: 9 March 2020
© Shanghai University and Springer-Verlag GmbH Germany, part of Springer Nature 2020

Abstract The in-situ TiB₂ particle reinforced aluminum matrix composites are materials that are difficult to machine, owing to hard ceramic particles in the matrix. In the milling process, the polycrystalline diamond (PCD) tools are used for machining these materials instead of carbide cutting tools, which significantly increase the machining cost. In this study, ultrasonic vibration method was applied for milling in-situ TiB₂/7050Al metal matrix composites using a TiAlN coated carbide end milling tool. To completely understand the tool wear mechanism in ultrasonic-vibration assisted milling (UAM), the relative motion of the cutting tool and interaction of workpiece-tool-chip contact interface was analyzed in detail. Additionally, a comparative experimental study with and without ultrasonic vibration was carried out to investigate the influences of ultrasonic vibration and cutting parameters on the cutting force, tool life and tool wear mechanism. The results show that the motion of the cutting tool relative to the chip changes periodically in the helical direction and the separation of tool and chip occurs in the transverse direction in one vibration period, in ultrasonic vibration assisted cutting. Large instantaneous acceleration can be obtained in axial ultrasonic vibration milling. The cutting force in axial direction is significantly reduced by 42%–57%, 40%–57% and 44%–54%, at different cutting speeds, feed rates and cutting depths, respectively, compared with

that in conventional milling. Additionally, the tool life is prolonged approximately 2–5 times when the ultrasonic vibration method is applied. The tool wear pattern micro-cracks are only found in UAM. These might be of great importance for future research in order to understand the cutting mechanisms in UAM of in-situ TiB₂/7050Al metal matrix composites.

Keywords Aluminum matrix composites · Ultrasonic vibration · Milling · Cutting force · Tool wear

1 Introduction

Particle reinforced metal matrix composites (PRMMCs), which are usually difficult to cut, are widely applied in aeronautics and astronautics owing to their high strength and good abrasion resistance [1–3]. However, the hard-ceramic reinforcements in the matrix result in significant tool wear, restricting the application of this material [4]. In the recent years, ultrasonic-vibration assisted milling (UAM) has been widely applied for machining the difficult-to-cut materials owing to the remarkable improvements in reducing the cutting force, decreasing tool wear, and extending tool life [5].

Lotfi et al. [6] developed a model to predict tool wear in ultrasonic assisted rotary turning. The model was validated by simulation and experiments, and the results showed that tool wear was reduced significantly. It was found that the heat transferred from chip to cutting tool was reduced due to the separation of the tool-chip interface. Peng et al. [7] analyzed the effect of elliptic ultrasonic vibration on tool wear. It was noted that the duration the tool participated in cutting was less than half cycle with elliptic ultrasonic vibration, reducing the tool wear considerably.

✉ Xiao-Fen Liu
xiaofl1987@mail.nwpu.edu.cn

¹ School of Mechanical Engineering, Northwestern Polytechnical University, Xi'an 710072, People's Republic of China

² School of Aeronautics and Astronautics, Sichuan University, Chengdu 610065, People's Republic of China

Subsequently, through experimental analysis and theoretical calculation, Soleimanimehr et al. [8] found out that the ratio of tool cutting time in one vibration period was 0.4555943. Nath et al. [9–11] proposed a tool-workpiece contact ratio and speed ratio to analyze the influences of the ultrasonic vibration parameters on the cutting force and tool wear. They concluded that reducing the tool-workpiece contact ratio and the speed ratio could significantly reduce the cutting force and tool wear.

Dong et al. [12] conducted a series of comparative experiments between ultrasonic vibration assisted turning and conventional turning for SiC_p/Al metal matrix composites (MMCs) with polycrystalline diamond (PCD) tools. The results showed that tool wear was significantly reduced by applying ultrasonic vibration. Liu et al. [13] studied the effects of cutting parameters on the cutting force in ultrasonic vibration turning of SiC_p/Al MMCs. The results indicated that the cutting force of ultrasonic vibration turning was much less than that of conventional turning. It was concluded that lower cutting velocity and larger cutting depth contributed to the reduction of the cutting force significantly. To gain a better understanding on the material removal processes during ultrasonic vibration assisted cutting of SiC_p/Al MMCs, Zheng et al. [14] and Zha et al. [15] carried out scratch tests with and without ultrasonic vibration. It was noted that the scratch force and friction coefficient in ultrasonic vibration was less than those in the traditional method. Zhou et al. [16] studied the effects of ultrasonic vibration on the cutting force and tool wear in rotary ultrasonic machining of SiC_p/Al MMCs. The experimental results indicated that the cutting force in rotary ultrasonic machining was reduced by an average of 13.86% compared with conventional machining.

From the above analysis, it can be inferred that the ultrasonic vibration method has been applied for machining ex-situ difficult-to-cut materials such as SiC_p/Al MMCs. The cutting force and tool wear can be significantly reduced by applying ultrasonic vibration.

The in-situ TiB₂ particle reinforced 7050 aluminum matrix composites (TiB₂/7050Al MMCs) are new variant of difficult-to-cut materials, which are different from ex-situ SiC_p/Al MMCs and conventional metallic materials in preparation and material properties.

At the beginning of the study on machinability of this material, Xiong et al. [17] conducted an experimental investigation on tool wear during milling of in-situ TiB₂/7050Al MMCs with uncoated carbide tools. It was found that the tools were worn out at the initial wear stage and hence, uncoated carbide tools were not suitable for machining in-situ TiB₂/7050Al MMCs. Subsequently, in the study of machinability of in-situ TiB₂/7050Al MMCs [18], TiAlN coated tools were used for machining. It was found that TiAlN coating material was easily worn out,

resulting in severe tool wear. Lin et al. [19] found that the tool wear had a significant effect on increasing the cutting force and on residual stress distribution. Hence, cutting tools have restricted the application of the in-situ TiB₂/7050Al MMCs. In order to study tool wear in depth, Jiang et al. [20] investigated the tool wear of different cutting tools (PCD, PCBN, and coated carbide tool), and it was concluded that PCD tool was the most suitable for cutting the in-situ TiB₂/7050Al MMCs owing to its superior hardness and wear resistance.

However, it is well known that the cost of PCD tool is very high, which is undesirable for industrial use. Hence, it is important to explore an advanced manufacturing technology to solve the problem of machinability of in-situ TiB₂/7050Al MMCs.

The current study is inspired by ultrasonic vibration assisted cutting, which has been found to have a significant influence on reducing tool wear and extending tool life. In this study, ultrasonic-vibration assisted milling (UAM) is applied for cutting TiB₂/7050Al MMCs. The motion of the cutting tool and separation between cutting tool and chip are analyzed. Comparative experiments have been carried out with and without ultrasonic vibration. To understand the influence of ultrasonic vibration, the effects of cutting parameters on cutting forces, tool wear, and tool life are analyzed.

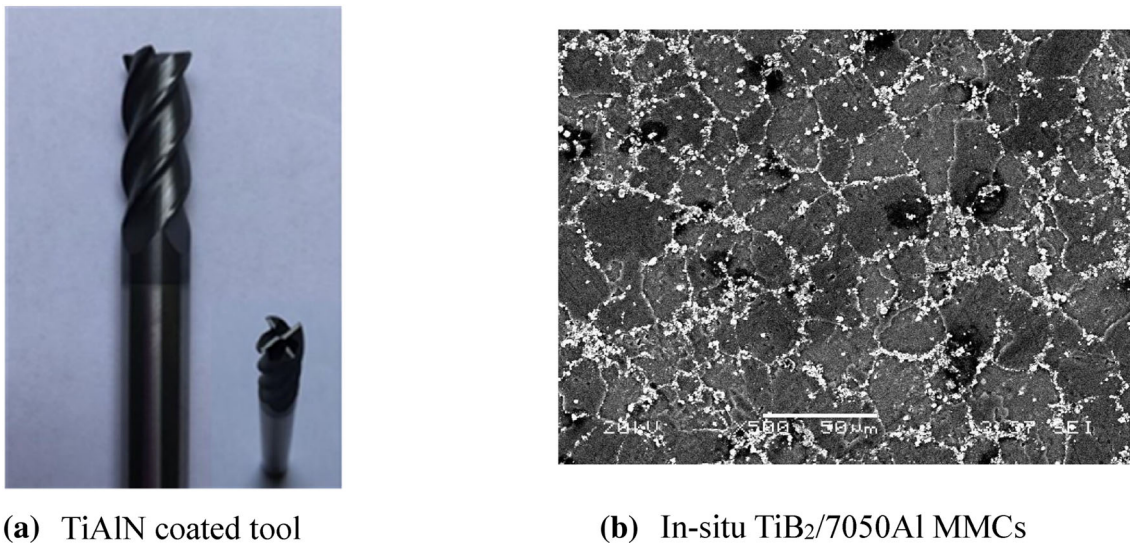
2 Experimental procedure

2.1 Tool and workpiece

In this study, the TiAlN coated carbide end milling tool and 6% (mass fraction) in-situ TiB₂/7050Al MMCs were used as shown in Fig. 1. The specifications of the tool and chemical content of the in-situ TiB₂/7050Al MMCs are listed in Tables 1 and 2, respectively.

2.2 Experimental design and measurement

A series of milling tests were conducted on a VMC-850 CNC machine with and without ultrasonic vibration under the same cutting conditions, i.e., down milling and dry cutting, which are presented in Fig. 2. The ultrasonic generator used was the SY2000, manufactured by Shaanxi Chao Ke Neng Electromechanical Technology Development Co. Ltd, whose vibration frequency was 22 kHz and was not adjustable. The vibration amplitude on the tip of the cutting tool was measured using a laser displacement meter LK-G5000 made by Keyence Co. Ltd (China). Measurement was performed before each experiment in order to ensure the optimum vibration state. In this study, the vibration amplitude was 4 μm. A set of orthogonal



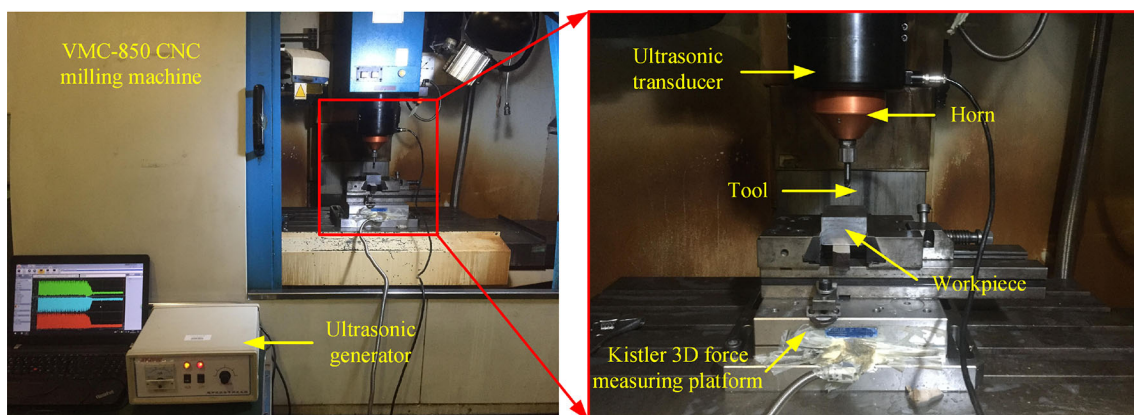
(a) TiAlN coated tool

(b) In-situ $\text{TiB}_2/7050\text{Al}$ MMCs**Fig. 1** Cutting tool and workpiece material**Table 1** Specifications of coated carbide milling tool

Diameter/mm	Rank angle/(°)	Nose radius/mm	Flank angle/(°)	Helix angle/(°)	Tooth
8	8	0.15	23	40	4

Table 2 Chemical content of the aluminum matrix (mass fraction, %)

Elements	Zn	Zr	Mg	Cu	Al
Content	6.30	0.11	2.30	2.20	Balanced

**Fig. 2** Milling test

cutting tests and single-factor tests were performed to investigate the influences of cutting parameters on the tool wear mechanism. The details of the cutting parameters are listed in Table 3.

In this study, the benchmark of failure was set such that when the flank wear approached 0.3 mm the cutting tool was worn out. The flank wear was observed using an automatic tool scanner (Alicona IFM-G4), after the

Table 3 Experiments parameters and levels

No.	Factor	Notation	Level		
			1	2	3
1	Cutting speed/(m·min ⁻¹)	v_s	25.12	50.24	75.36
2	Feed rate/(mm·z ⁻¹)	f_z	0.10	0.25	0.40
3	Cutting depth/mm	a_p	0.20	0.40	0.60

operation of the cutting tool for a certain time duration. The cutting force was measured using a Kistler 3D force-measuring platform during milling. The measurement of cutting force of each flute was repeated twice, and the average of three flutes was reported. For each cutting test, the measurement of flank wear was repeated thrice and the average values were obtained. Additionally, the cutting time of each tool corresponding to the flank wear approaching 0.3 mm was reported. After experiments, the tools were examined using a scanning electron microscope (VEGA 3 LMU SEM-EDS).

3 Results and discussions

3.1 Analysis of UAM

To effectively understand the process of tool wear in UAM, the relative motion between the cutting tool and workpiece was analyzed. In UAM, ultrasonic sinusoidal wave signals were imparted to the cutting tool in the axial direction during conventional milling (CM) process, as shown in Fig. 3.

Due to ultrasonic vibration, the trajectory of the cutting tool in UAM process can be described as follows

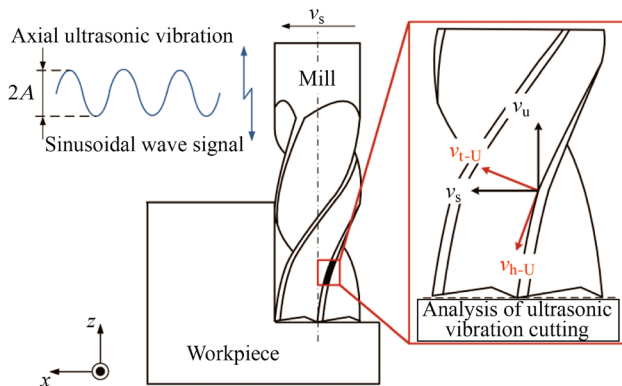


Fig. 3 Schematics of ultrasonic vibration cutting principle (A is the vibration amplitude (μm))

$$\begin{cases} x = v_s t, \\ z = A \sin(2\pi f t), \end{cases} \quad (1)$$

where v_s is the cutting speed, t cutting time, A and f the vibration amplitude and frequency, respectively. According to Eq. (1), the motion of the cutting tool can be expressed as

$$\begin{cases} v_x = v_s, \\ v_z = 2\pi A f \cos(2\pi f t). \end{cases} \quad (2)$$

It can be observed that the total velocity consists of two components, the cutting speed and vibration velocity. In order to understand the effect of ultrasonic vibration on the cutting process, a set of rectangular axes are constructed. The cutting speed v_x and vibration velocity v_z are both resolved into rectangular components, as shown in Fig. 3. The rectangular components can be expressed as

$$\begin{cases} v_{h-U} = v_s \sin \beta - 2\pi A f \cos \beta \cos(2\pi f t), \\ v_{t-U} = v_s \cos \beta + 2\pi A f \sin \beta \cos(2\pi f t), \end{cases} \quad (3)$$

where β is the helix angle. v_{h-U} is the velocity in helix direction, and it causes abrasion between the cutting tool and workpiece. v_{t-U} is the velocity in transverse direction, and it creates intermittent cutting. From Eq. (3), the motion of the cutting tool is determined by the vibration frequency, vibration amplitude, and cutting speed. Furthermore, the acceleration of the cutting tool can be obtained by differentiating the components of the cutting velocity as

$$\begin{cases} a_{h-U} = 4\pi^2 f^2 A \sin(2\pi f t) \cos \beta, \\ a_{t-U} = -4\pi^2 f^2 A \sin(2\pi f t) \sin \beta. \end{cases} \quad (4)$$

In order to analyze the kinematics of the cutting tool and the mechanism of intermittent cutting, a set of experimental parameters ($f = 20$ kHz, $A = 5$ μm , $v_s = 25.12$ m/min) are selected to plot the speed and acceleration curves as shown in Fig. 4. In Fig. 4, v_{h-C} and v_{t-C} are the velocities in helix and transverse directions, respectively, in the CM process.

It may be noted that the velocity of the cutting tool varies from time to time in a vibration period, and sub-zero velocity is achieved during the UAM process. However, the velocity of the cutting tool does not change and is more than zero during the CM process, which can be observed in Fig. 4a. The acceleration of the cutting tool is generated due to the assistance of ultrasonic vibration, which is shown in Fig. 4b. It also changes over time in the vibration period and its maximum value is significantly greater than gravitational acceleration.

For analyzing the kinematics of the cutting tool, the cutting velocity curve is divided into five parts in a vibration period, as shown in Fig. 5.

From Fig. 5a, it can be observed that the transverse velocity v_{t-U} and the helix velocity v_{h-U} are both greater

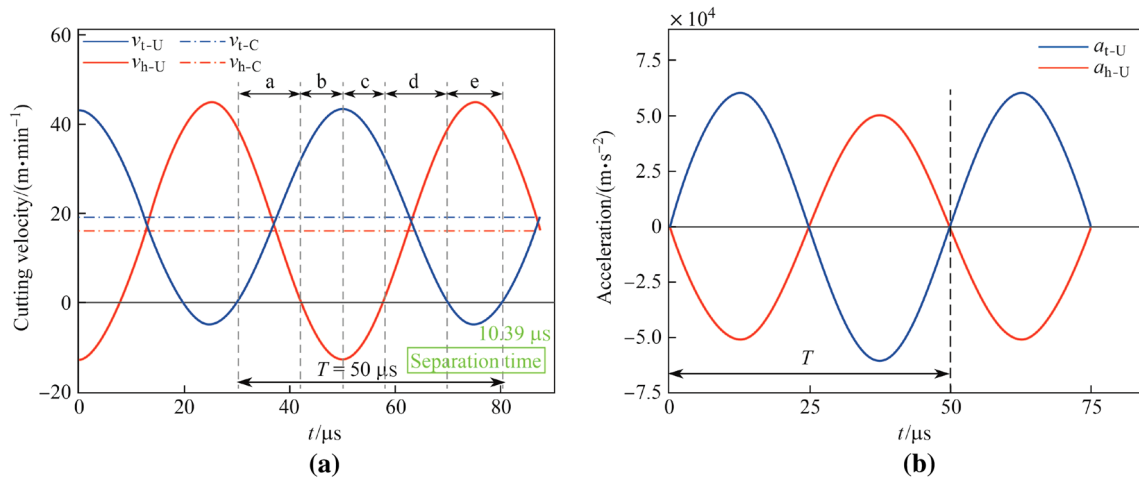


Fig. 4 Analyze the kinematics of cutting tool **a** cutting velocity curve **b** acceleration curve

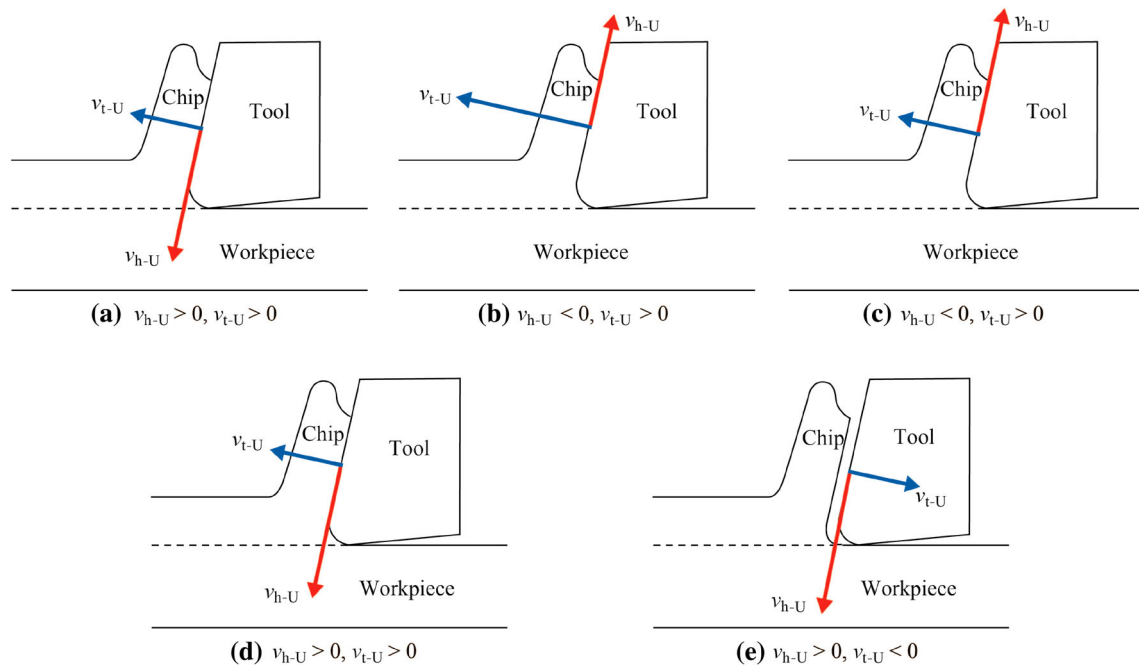


Fig. 5 Schematics of the physical states of stages **a-e** in Fig. 4

than zero but show opposite behavior in stage a (see Fig. 4a). The former increases, but the latter decreases to zero. In stage b (see Fig. 4a), the transverse velocity v_{t-U} increases further and attains the maximum value. The direction of the helix velocity v_{h-U} changes and the magnitude increases to the maximum value. From stage a to b (see Fig. 4a), the cutting tool maintains contact with the chip, but the relative motion between them changes.

From Figs. 4a and 5c, d, it can be observed that the transverse velocity v_{t-U} decreases from the maximum to zero and that the helix velocity v_{h-U} decreases from the maximum to zero and then increases. In this process, the direction of the helix velocity v_{h-U} changes again.

In the stage e, from Figs. 4a and 5e, it can be observed that the helix velocity v_{h-U} increases to the maximum and then decreases. The transverse velocity v_{t-U} is less than zero, indicating that its direction changes. Its magnitude increases first and then decreases, indicating that, at first, the cutting tool moves away from the chip and then moves towards it.

Based on the above analysis, the helix velocity v_{h-U} changes from negative values in the stages a–b to positive values in stages c–d, indicating that the relative motion direction changes twice in one vibration period. The transverse velocity v_{t-U} attains a positive value in stage a–d, which indicates that the cutting tool maintains contact with

the chip. However, the transverse velocity v_{t-U} is less than zero in stage e, which indicates that separation occurs between the cutting tool and the chip.

However, the helix velocity v_{h-C} and transverse velocity v_{t-C} are constant during the CM process. Clearly, in the UAM process, tool-chip contact changes periodically owing to the application of ultrasonic vibration.

It may be noted that the separation of the tool-chip does not always occur and that it has to adhere to a certain condition. Kim and Choi [21] inferred that tool-chip separation occurred when the cutting velocity was below the critical cutting velocity ($v_c < 2\pi fA$) in feed ultrasonic vibration cutting. However, because the axial ultrasonic vibration is significantly different from feed ultrasonic vibration, the critical cutting velocity criterion is not suitable for axial ultrasonic vibration cutting. According to the analysis of motion of tool-chip, the condition of separation is that v_{t-U} is less than zero, which signifies that if the cutting speed $v_s < 2\pi fA \tan\beta$, the tool-chip separation occurs. Hence, the critical cutting speed v_c that satisfies the condition of separation is $v_c = 2\pi fA \tan\beta$.

According to Verma, the contact time (T_c) is expressed as [22]

$$T_c = \frac{1}{f} - \frac{1}{\pi f} \arccos\left(\frac{v_s \cot\beta}{2\pi fA}\right). \quad (5)$$

The separation time (T_s) in one vibration period, which is calculated according to Eq. (5), is determined as

$$T_s = \frac{1}{\pi f} \arccos\left(\frac{v_s \cot\beta}{2\pi fA}\right). \quad (6)$$

It can be observed that the contact time of tool-chip is determined by the cutting speed with ultrasonic vibration of a certain amplitude and frequency. Under this set of cutting parameters ($f = 20$ kHz, $A = 5$ μm , $v_s = 25.12$ m/min), the separation time is 10.39 μs , as shown in Fig. 4.

From this analysis, it can be observed that the cutting tool performs a different machining process in UAM compared to CM. The different characteristics significantly impact the cutting force, tool wear mechanism, and tool life.

3.2 Cutting force

In the cutting process, cutting force is an important factor related to tool wear [23]. In this study, the instant cutting force is presented in Fig. 6. F_x , F_y and F_z refer to the horizontal, vertical, and axial forces in UAM and CM, respectively.

It can be observed that the peak value of instant cutting force in UAM is much less than that in CM. The maximum cutting force of each tooth is relative stable in UAM but shows an obvious fluctuation in the CM process.

Additionally, the cutting force is represented by a single continuous curve in CM, while it is formed by a dense pulse beam in UAM.

In order to analyze the influences of cutting parameters on the cutting force, the average cutting force is shown in Fig. 7. It is clear that the cutting force in UAM is less than that in CM. There is a significant reduction of F_z in UAM by 42%–57%, 40%–57% and 44%–54% at different cutting speeds, feed rates and cutting depths, respectively, compared with that in CM process. This may be attributed to the periodic variation of the tool-chip contact behavior due to the imposed ultrasonic vibration. From the motion of the cutting tool, high impact energy is produced because of the large instantaneous acceleration that decreases the plastic deformation in the shear zone. The cutting tool separates from the chip twice in one vibration period, decreasing the friction coefficient on the tool-chip interface. Additionally, it has been found earlier that periodic separation of tool-chip reduces the cutting force [24]. Furthermore, Jin and Murakawa [25] and Mitrofanov et al. [26] inferred that the reason for cutting force reduction was the reduction in friction between the cutting tool and workpiece in UAM. It can be observed that the trend of the effects of cutting parameters on the cutting force are different in the two methods. From Fig. 7a, with the increase of cutting speed, the cutting force components F_x and F_z decrease in the CM process while there is minimal change observed in UAM. This may be because the volume of material removed per unit time decreases, reducing the extrusion between the cutting tool and workpiece in CM. The material removal depends on the impact energy, which is determined by the vibration frequency and amplitude in UAM. It can be inferred from Figs. 7a–c that there is insignificant variation in the cutting force F_z at different cutting speeds, feed rates and cutting depths in the UAM process because of the same ultrasonic vibration imposed in the axial direction. The cutting force F_x increases with the increase of feed rate and cutting depth because the removed material volume increases in the UAM process.

3.3 Tool life

Cutting speed, feed rate and cutting depth have an important influence on the tool life in UAM and CM, as shown in Fig. 8. In this study, the tool life is defined as the time taken for the flank wear of the coated carbide milling tool to approach 0.3 mm in the two cutting methods.

It can be observed that the tool life of UAM is greater than that of CM. This may be because of the reduction in both the cutting force and tool-chip contact time with the application of ultrasonic vibration, thereby mitigating tool wear. Cutting speed plays an important role in tool life improvement. It is interesting to note that the tool life is

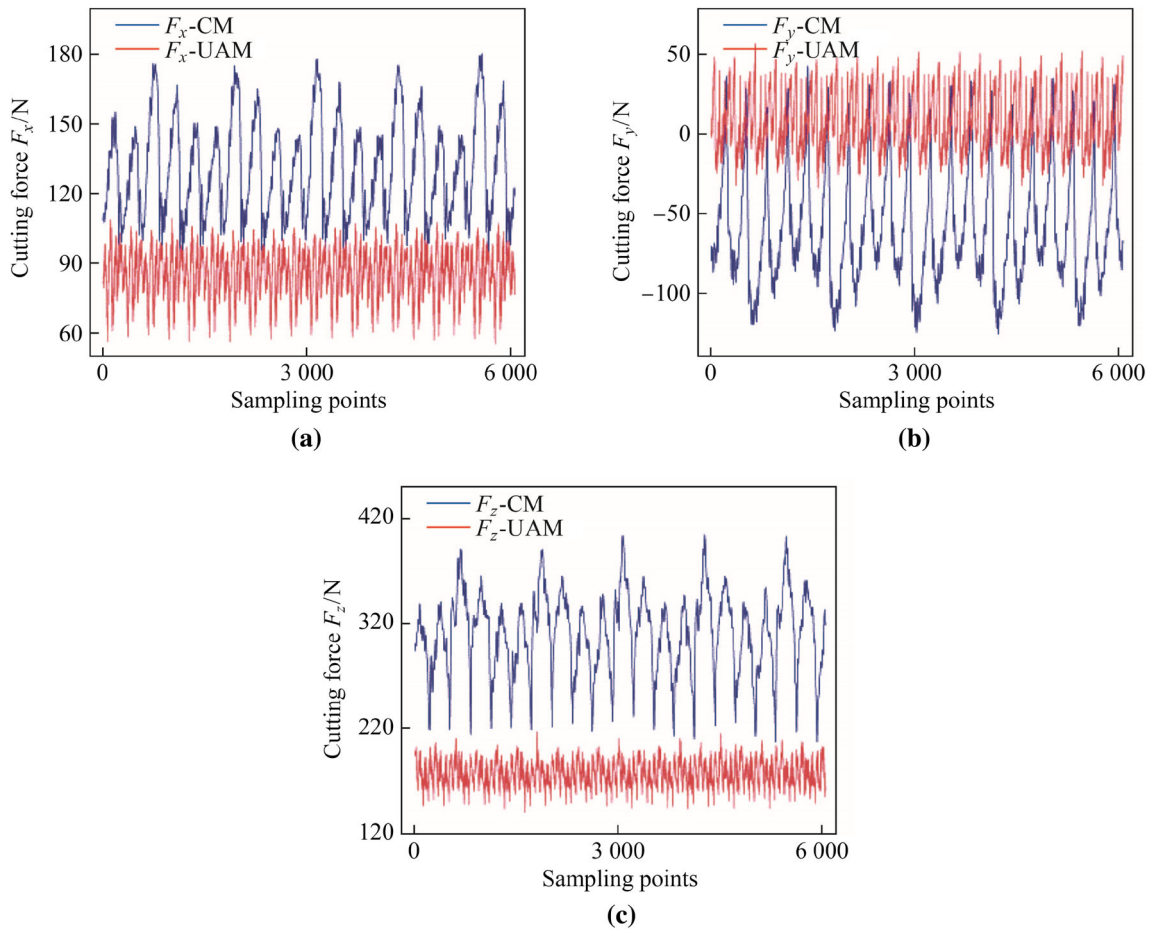


Fig. 6 Instant cutting forces

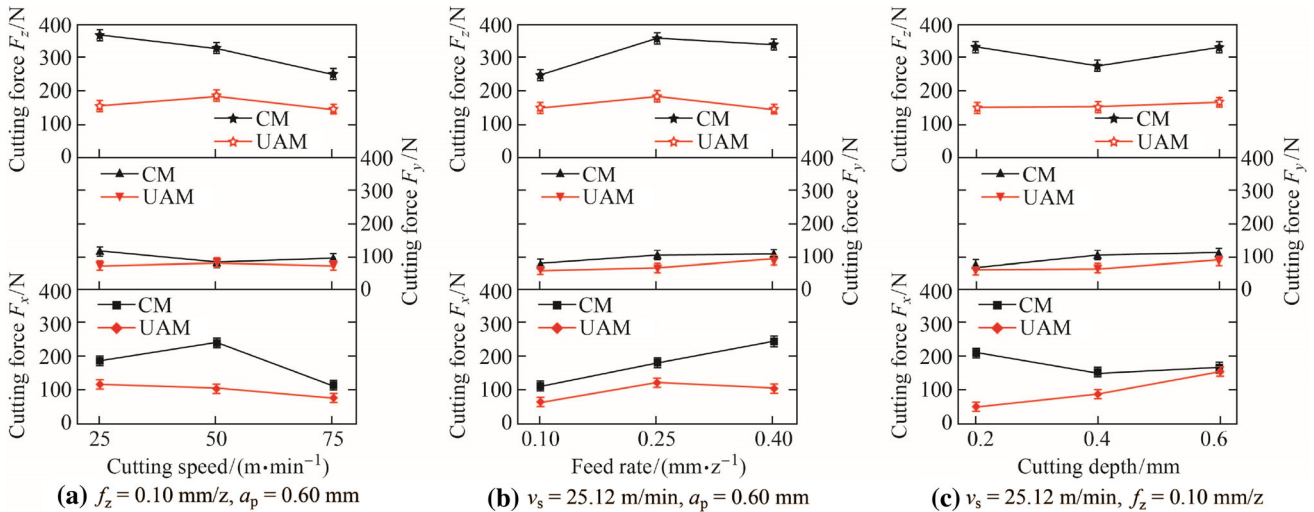


Fig. 7 Average cutting forces (f_z is feed rate and a_p is cutting depth)

significantly longer in UAM when the cutting speed is less than 50 m/min. Additionally, it is close to the tool life in CM when the cutting speed is more than 50 m/min. The possible reason is when the cutting speed is below the

critical value, the cutting tool can separate from the chip, based on the analysis in Sect. 3.1. In a related study, it was observed that the separation of tool-chip could improve the aerodynamic lubrication, decreasing the friction between

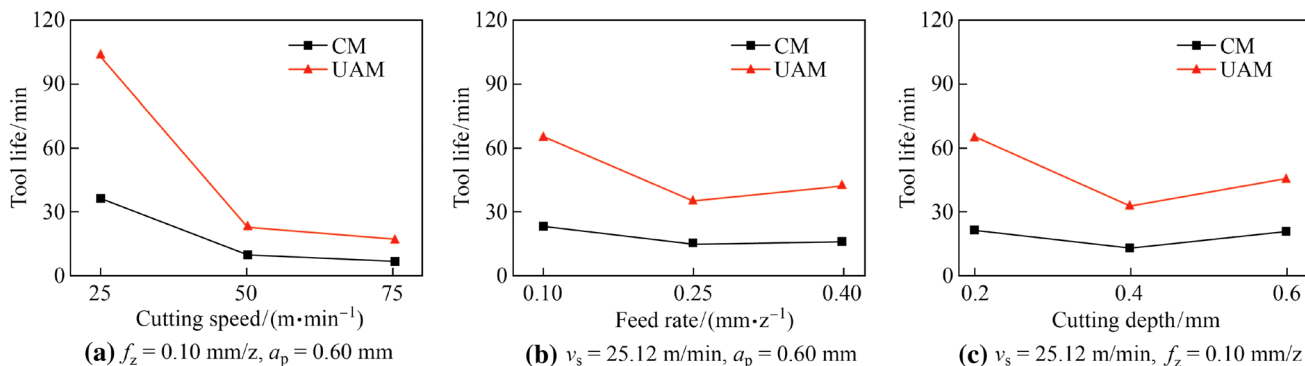


Fig. 8 Tool life in UAM and CM

the tool and workpiece [24]. Hence, the tool life is extended due to the reduction in the contact time and friction because of ultrasonic vibration.

In order to completely understand the effect of cutting parameters on tool life, a regression model has been developed as follows

$$T_{UAM} = 10\,601v_s^{-1.65024}f_z^{-0.23452}a_p^{-0.1719}, \tag{7}$$

$$T_{CM} = 5\,664v_s^{-1.69885}f_z^{-0.36883}a_p^{-0.21784}, \tag{8}$$

where T_{UAM} and T_{CM} are the tool life in UAM and CM, respectively.

Tables 4 and 5 show the analysis of variance (ANOVA) results of Eqs. (7) and (8). It can be observed that the regression model can be employed to analyze the relationship between the tool life and cutting parameters. It is found from the equations that cutting speed has the most significant effect on the tool life, followed by feed rate and cutting depth, in both UAM and CM, which is consistent with the analysis of Sect. 3.1 and the results of Sect. 3.3.

To compare the tool life in UAM and CM, the ratio of tool life (R) is defined as

$$R = \frac{t_{UAM}}{t_{CM}}, \tag{9}$$

where t_{UAM} and t_{CM} are the tool lives in UAM and CM, respectively. Figure 9 presents the comparison results of the experiments. It is observed that the tool life in UAM is extended significantly.

It is found that the tool life in UAM is approximately 2–5 times longer than that in CM. Clearly, ultrasonic

Table 5 ANOVA results of Eq. (8) for CM

	DF	Sum of squares	Mean square	F	Prob > F
Model	3	5.838 03	1.946 01	9.970 98	0.014 98
Error	5	0.975 84	0.195 17		
Total	8	6.813 87			

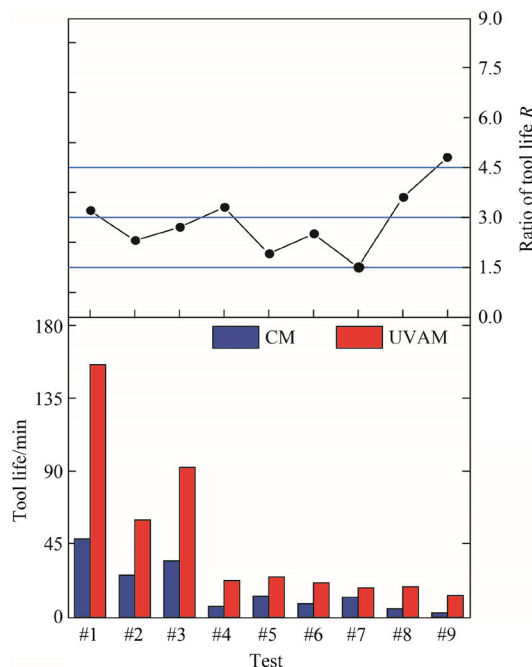


Fig. 9 Comparison results of tool life between UAM and CM

Table 4 ANOVA results of Eq. (7) for UAM

	DF	Sum of squares	Mean square	F	Prob > F
Model	3	5.261 74	1.753 91	16.430 79	0.005 07
Error	5	0.533 73	0.106 75		
Total	8	5.795 46			

vibration contributes to extending the tool life during machining TiB₂/Al MMCs.

3.4 Tool wear progression

For understanding the effect of ultrasonic vibration on improving the tool life, tool wear progression is analyzed in UAM and CM, which is shown in Fig. 10.

It can be clearly observed that the tool flank wear progression in UAM is considerably different from that in CM. However, in this study, both these are different from normal tool wear progression. Generally, in the cutting process, typical tool wear progression comprises an initial wear stage, normal wear stage, and rapid wear stage. For a better understanding of the tool wear progression, linear fitting is adopted to approximate the characteristics of tool wear, which are marked as A, B and C in Fig. 11. A, B and C represent linear wear progress, normal wear progress and rapid wear progress, respectively.

It can be observed that tool wear progress in CM shows a quick linear increase, indicating that tool wear is quite severe and rapid. This also demonstrates that the TiAlN coated carbide tool is unsuitable for CM of in-situ TiB₂/Al MMCs. As a result, the wear stage progresses linearly. However, the progression of wear in UAM is considerably different from that in CM, which comprises two wear

stages. This indicates that the tool wear in UAM is much lesser and the tool is worn out relatively slowly, compared to the tool wear in CM. The cutting time and cutting force decrease significantly, which is the responsible for the slow wearing of the cutting tool. Zhu and Zhang [27] proposed a tool wear model, which indicated that as the cutting time reduced, the tool wear decreased. It can also be observed that the tool wear experiences a normal wear stage and then a rapid wear stage in UAM. Additionally, the tool wear progresses to the rapid stage at approximate 88 min as shown in Fig. 11a. This could be because the effective cutting time and the friction of the tool-chip is reduced with ultrasonic vibration, as analyzed in Sect. 3.1. Another case is when the tool wear experiences a rapid wear stage first and then the normal wear stage, as shown in Figs. 11b, c. The wear rate in the two figures is similar. These results indicate that large feed rate and cutting depth result in rapid tool wear. This is because more material is removed at large feed rate and cutting depth, resulting in the increase in cutting force. Based on the kinematic analysis of the cutting tool, when the cutting speed exceeds the critical value, the ultrasonic vibration cutting process becomes the same as conventional cutting. The cutting speed is

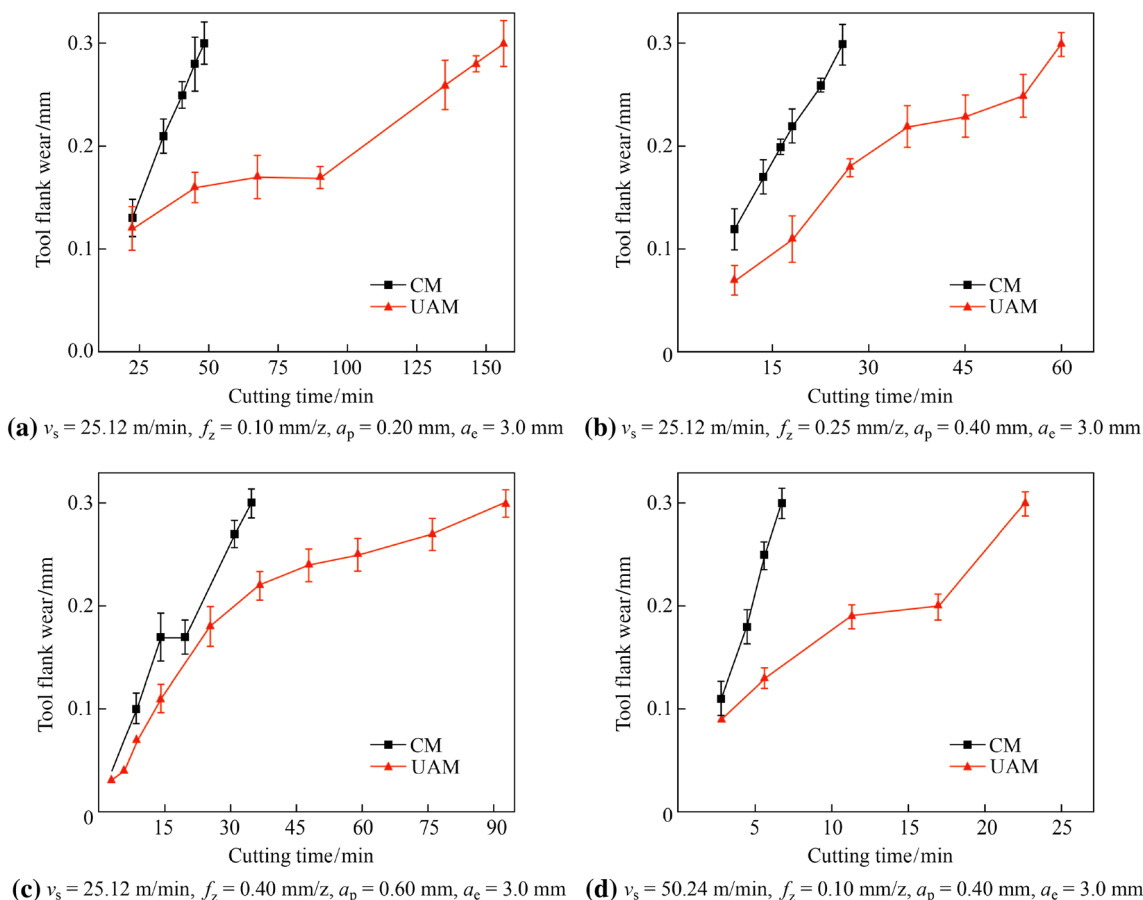


Fig. 10 Tool wear progression

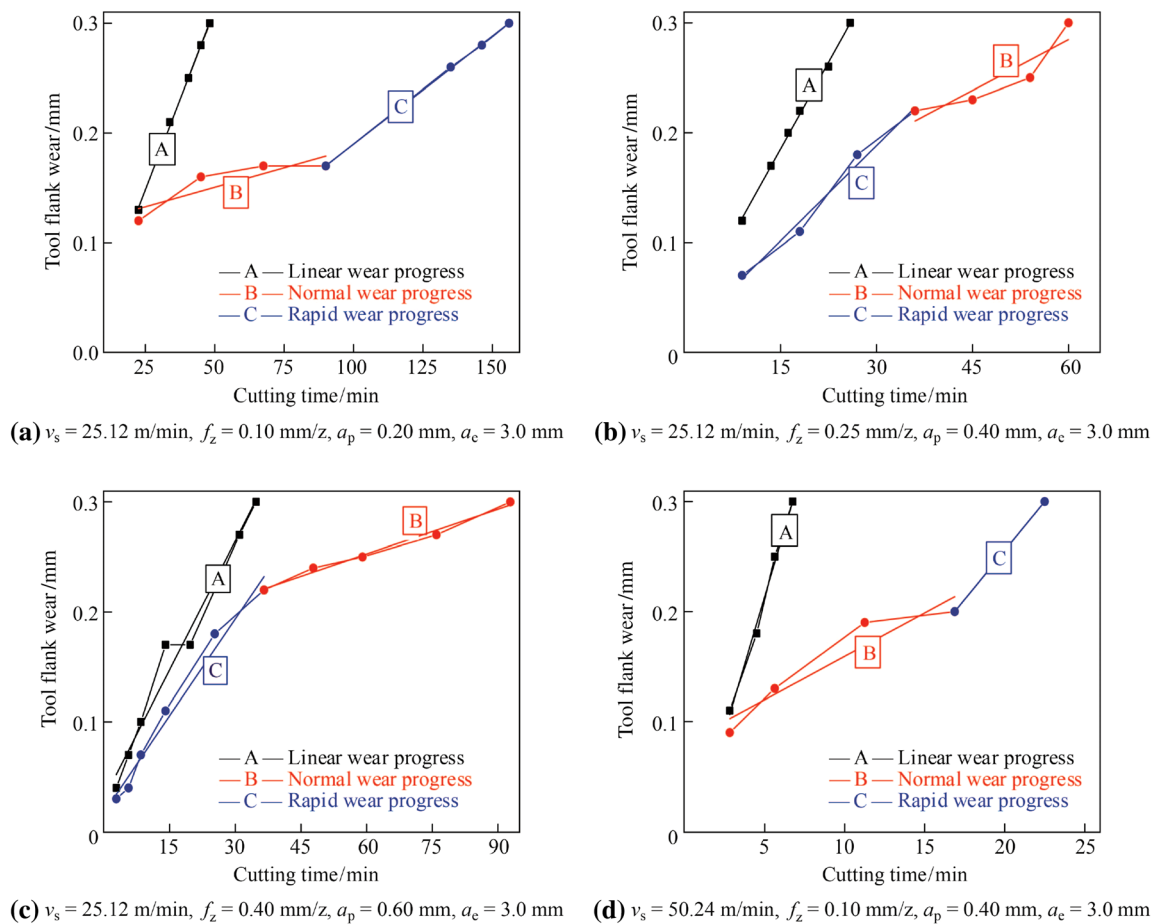


Fig. 11 Fitting tool wear progression under different combinations of cutting parameters

50.24 m/min, which is greater than the critical cutting speed as presented in Fig. 11d. However, it can be observed that tool wear in UAM is not the same as that in CM. This may be because the regular ultrasonic vibration results in changing the irregular vibration of the machine tool system. As a result, applying UAM is superior for mitigating tool wear while machining in-situ TiB₂/Al MMCs.

3.5 Tool wear mechanisms

Figures 12 and 13 show the SEM topographies of tools worn out in CM and UAM, respectively.

From Fig. 12a and 13a, abrasive wear is produced on the tools, machining in-situ TiB₂/Al MMCs, with and without ultrasonic vibration. It can be observed that TiAlN coating is removed for the coated carbide tools, and small grooves can be observed on the flank of tools, as several particles in the in-situ TiB₂/Al MMCs are extremely hard and abrasive; hence, the flank faces of the tools are easily destroyed. Additionally, the grooves created on the surface of the cutting tool in UAM are smaller, as the interaction of chip-

tool-workpiece has been altered because of the ultrasonic vibration. It is known that the relative motion of the cutting tool to the chip varies periodically in UAM, resulting in changing the friction of the interface of tool-chip. Using the ultrasonic vibration, rubbing and ploughing between the flank face of the cutting tool and the workpiece is reduced.

From Figs. 12b, c and 13b, c, it can be observed that the cutting tool suffers from peeling, tipping, chipping wear during milling in-situ TiB₂/Al MMCs, with and without ultrasonic vibration. However, the surface topography of the tool wear is quite different in CM and UAM. The material of the cutting tool is peeled with the configuration of a flake, and the surface appearance is flat in the CM process. While the material falls off as powder, the surface appearance shows granular regions in UAM. This may be because of different interactions occurring between the cutting tool and the workpiece. The cutting tool suffers from extrusion and alternate stress when the material is removed during CM process. However, due to imposing ultrasonic vibration on the cutting tool, its motion is

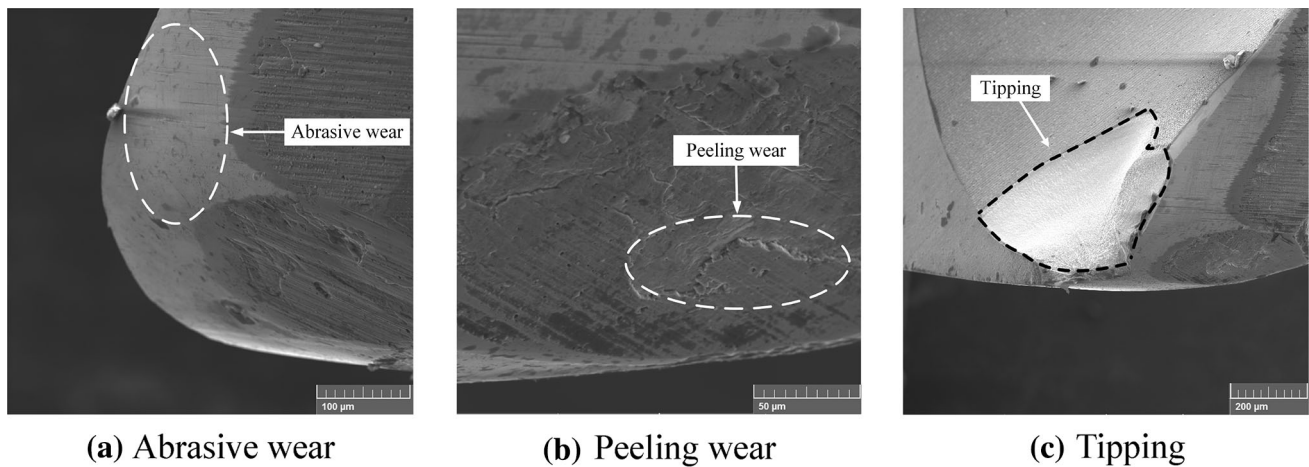


Fig. 12 SEM topographies of tools worn out for conventional milling

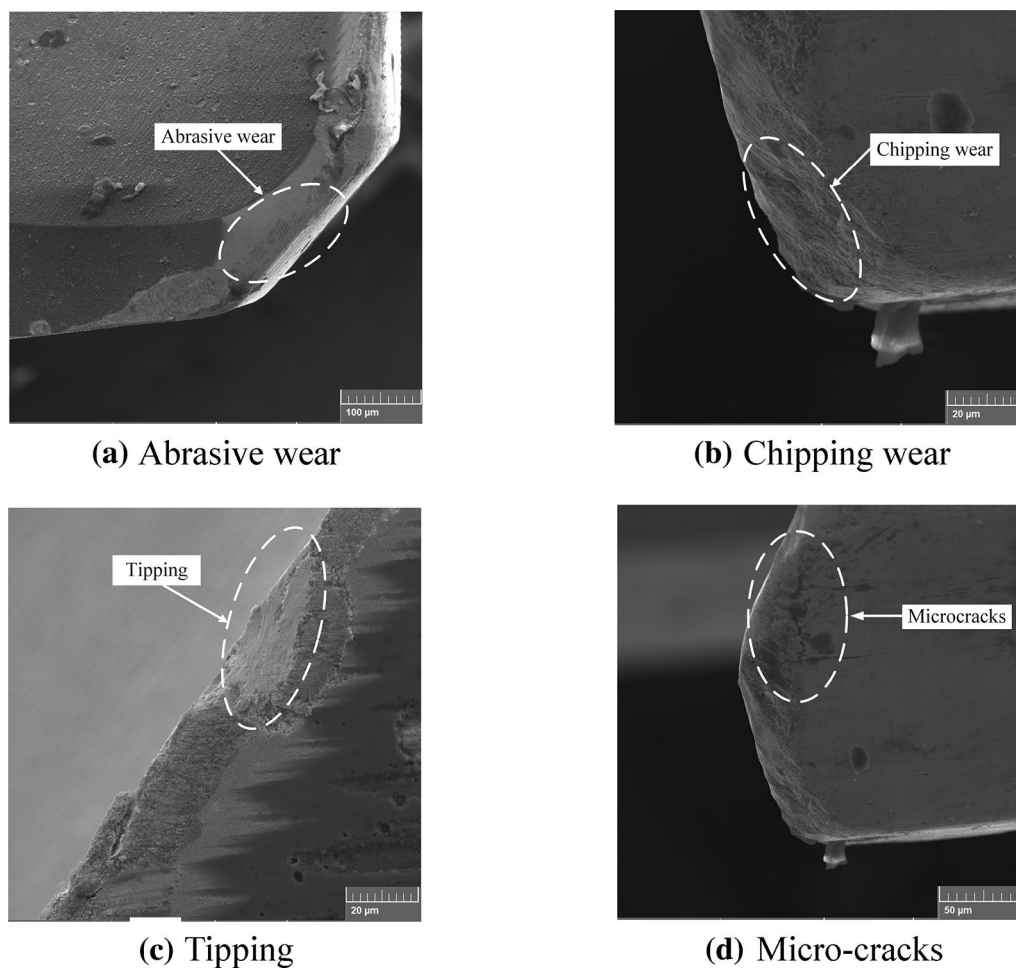


Fig. 13 SEM topographies of tools worn out for UAM

changed periodically. The cutting tool mainly bears the alternate stress, resulting in microchipping in UAM.

Furthermore, micro-cracks are found on the surface of the worn-out tools for UAM, which is shown in Fig. 13d.

With the application of ultrasonic vibration, the velocity and acceleration of the cutting tool is changed periodically, as analyzed in Sect. 3.1. Consequently, the cutting tool is subjected to impulsive and alternate loads, which result in

alternate stress. This leads to the generation of microcracks on the cutting edge. Shen and Xu [23] have explained that pulse-like cutting forces caused by the imposed ultrasonic vibration induce a strong instantaneous kinetic energy leading to macro or micro-cracks. Hence, the microcrack formation on the cutting edge results primarily from the alternate stress in UAM.

4 Conclusions

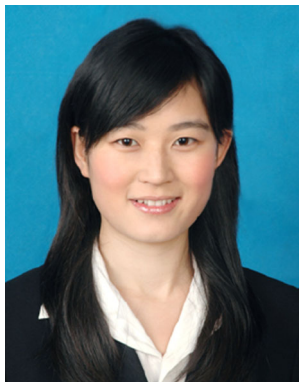
In the present study, the effects of ultrasonic vibration on the tool life and wear mechanisms have been investigated by theoretical analysis and experimentation during the milling of in-situ TiB₂/7050Al MMCs, with and without ultrasonic vibration. From the analysis and results, the conclusions obtained are as follows. (i) Due to ultrasonic vibration, the relative motion of the cutting tool is changed, and periodic variation of cutting velocity and high instantaneous acceleration is generated in the UAM process, resulting in material removal mechanisms, which are different from those in the CM process. (ii) The experimental results reveal that the cutting force of UAM is much less than that of CM. Particularly, there is a significant reduction of the axial cutting force F_z by 42%–57% at different cutting speeds. (iii) It is found that UAM can dramatically extend tool life even when coated carbide tools are used, which are not suitable for cutting in-situ TiB₂/7050Al MMCs in CM. Compared to CM, in UAM, the tool life is approximately improved 2–5 times. (iv) The tool wear progression in UAM and CM is quite different from the normal tool wear progression. The cutting tool in CM only suffers from linear wear progression, indicating that the cutting tool is worn out rapidly. However, the cutting tool in UAM is first subjected to the normal wear stage and then the rapid wear stage or vice versa, indicating that tool service life is significantly increased. (v) From the analysis of tool worn topographies, it can be observed that the main tool wear mechanisms consist of abrasive wear, peeling wear, and tipping. Microcracks occur only in UAM due to the alternate stress. However, further research is required to obtain a better understanding of the machinability of in-situ TiB₂/7050Al MMCs with axial UAM. The material removal mechanisms, surface integrity, cutting force, and temperature models will be studied in the future.

Acknowledgements This work is sponsored by the National Natural Science Foundation of China (Grant No. 51775443), the Innovation Foundation for Doctor Dissertation of Northwestern Polytechnical University (Grant No. CX201829), and the National Science and Technology Major Project (Grant No. 2017-VII-0015-0111).

References

- Przestacki D (2014) Conventional and laser assisted machining of composite A359/20SiC_p. Proc CIRP. <https://doi.org/10.1016/j.procir.2014.03.029>
- Teng XY, Huo DH, Shyha I et al (2018) An experimental study on tool wear behaviour in micro milling of nano Mg/Ti metal matrix composites. Int J Adv Manuf Technol 96:2127–2140
- Geng JW, Liu G, Wang FF et al (2017) Microstructural correlated damage mechanisms of the high-cycle fatigued in-situ TiB₂/Al-Cu-Mg composite. Mater Des 135:423–438
- Xiang JF, Pang SQ, Xie LJ et al (2018) Investigation of cutting forces, surface integrity, and tool wear when high-speed milling of high-volume fraction SiC_p/Al6063 composites in PCD tooling. Int J Adv Manuf Technol 98:1237–1251
- Brehl DE, Dow TA (2008) Review of vibration-assisted machining. Precis Eng 32:153–172
- Lotfi M, Amini S, Aghaei M (2018) 3D FEM simulation of tool wear in ultrasonic assisted rotary turning. Ultrasonics 88:106–114
- Peng Y, Liang Z, Wu Y et al (2012) Effect of vibration on surface and tool wear in ultrasonic vibration-assisted scratching of brittle materials. Int J Adv Manuf Technol 59:67–72
- Soleimanimehr H, Nategh MJ, Najafabadi AF et al (2018) The analysis of the Timoshenko transverse vibrations of workpiece in the ultrasonic vibration-assisted turning process and investigation of the machining error caused by this vibration. Precis Eng 54:99–106
- Nath C, Rahman M, Andrew SSK (2007) A study on ultrasonic vibration cutting of low alloy steel. J Mater Process Technol 192–193:159–165
- Nath C, Rahman M (2008) Effect of machining parameters in ultrasonic vibration cutting. Int J Mach Tool Manuf 48:965–974
- Nath C, Rahman M, Neo KS (2009) Machinability study of tungsten carbide using PCD tools under ultrasonic elliptical vibration cutting. Int J Mach Tool Manuf 49:1089–1095
- Dong GJ, Zhang HJ, Zhou M et al (2013) Experimental investigation on ultrasonic vibration-assisted turning of SiC_p/Al composites. Mater Manuf Process 28:999–1002
- Liu CS, Zhao B, Gao GF et al (2002) Research on the characteristics of cutting force in the vibration cutting of a particle-reinforced metal matrix composites SiC_p/Al. J Mater Process Technol 129:196–199
- Zheng W, Wang YJ, Zhou M et al (2018) Material deformation and removal mechanism of SiC_p/Al composites in ultrasonic vibration assisted scratch test. Ceram Int 44:15133–15144
- Zha HT, Feng PF, Zhang JF et al (2018) Material removal mechanism in rotary ultrasonic machining of high-volume fraction SiC_p/Al composites. Int J Adv Manuf Technol 97:2099–2109
- Zhou M, Wang M, Dong GJ (2016) Experimental investigation on rotary ultrasonic face grinding of SiC_p/Al composites. Mater Manuf Process 31:673–678
- Xiong YF, Wang WH, Jiang RS et al (2016) Tool wear mechanisms for milling in situ TiB₂ particle-reinforced Al matrix composites. Int J Adv Manuf Technol 86:3517–3526
- Xiong YF, Wang WH, Jiang RS et al (2018) Machinability of in situ TiB₂ particle reinforced 7050Al matrix composites with TiAlN coating tool. Int J Adv Manuf Technol 97:3813–3825
- Lin KY, Wang WH, Jiang RS et al (2019) Effect of tool nose radius and tool wear on residual stresses distribution while turning in situ TiB₂/7050 Al metal matrix composites. Int J Adv Manuf Technol 100:143–151
- Jiang RS, Wang WH, Song GD et al (2016) Experimental investigation on machinability of in situ formed TiB₂ particles reinforced Al MMCs. J Manuf Process 23:249–257

21. Kim JD, Choi IH (1998) Characteristics of chip generation by ultrasonic vibration cutting with extremely low cutting velocity. *Int J Adv Manuf Technol* 14:2–6
22. Verma GC, Pandey PM, Dixit US (2018) Modeling of static machining force in axial ultrasonic-vibration assisted milling considering acoustic softening. *Int J Mech Sci* 136:1–16
23. Shen XH, Xu GF (2018) Study of milling force variation in ultrasonic vibration-assisted end milling. *Mater Manuf Process* 33:644–650
24. Chen G, Ren CZ, Zou YH et al (2019) Mechanism for material removal in ultrasonic vibration helical milling of Ti-6Al-4V alloy. *Int J Mach Tool Manuf* 138:1–13
25. Jin M, Murakawa M (2001) Development of a practical ultrasonic vibration cutting tool system. *J Mater Process Technol* 113:342–347
26. Mitrofanov AV, Ahmed N, Babitsky VI et al (2005) Effect of lubrication and cutting parameters on ultrasonically assisted turning of Inconel 718. *J Mater Process Technol* 162–163:649–654
27. Zhu KP, Zhang Y (2019) A generic tool wear model and its application to force modeling and wear monitoring in high speed milling. *Mech Syst Signal Process* 115:147–161



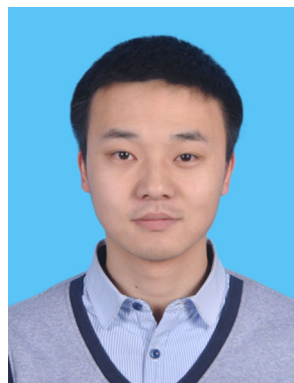
Xiao-Fen Liu received the M.S degree in Mechanical Engineering from Lanzhou University of Technology in 2014. Now she is a Ph.D student at Northwestern Polytechnical University. Her research interest is ultrasonic vibration assisted cutting of difficult-to-machined materials.



Wen-Hu Wang received the Ph.D degree in Aeronautical and Astronautical Manufacturing Engineering from Northwestern Polytechnical University in 2007. Now he is a Professor at Northwestern Polytechnical University. His research interests include multi-coordinate NC machining and composite material forming.



Rui-Song Jiang received the Ph.D degree in Aeronautical and Astronautical Manufacturing Engineering from Northwestern Polytechnical University in 2011. Now he is an Associate Professor at Sichuan University. His research interests include basic cutting theory of difficult-to-machined materials and 3D printing technology.



Yi-Feng Xiong received the Ph.D degree in Aeronautical and Astronautical Manufacturing Engineering from Northwestern Polytechnical University in 2019. Now he is a Post-Doc at Northwestern Polytechnical University. His research interests include basic cutting theory of difficult-to-machined materials and ultrasonic vibration assisted cutting.



Kun-Yang Lin is a Ph.D student in Northwestern Polytechnical University. His research focuses on the precision cutting technology of metal matrix composites.